ISBN: 978-628-96613-3-0. ISSN: 2414-6390. Digital Object Identifier: https://dx.doi.org/10.18687/LACCEI2026.1.1.2294

Multicriteria Ranking and Micromechanical Preselection of Natural-based Composite Families for Circular Material Pathways

Librada Del Carmen Nieto Jaén[1]; Karla María Aguirre Barría[1]; Maria De Los Ángeles Ortega Del Rosario[1,2,3,4]; Melany Nicole Pérez Medina[1]

[1]Research Group in Design, Manufacturing and Materials (DM+M), School of Mechanical Engineering, Universidad Tecnológica de Panamá, Panama City 0819-07289, Panama, librada.nietojaen@gmail.com, librada.nietojaen@gmail.com, *maria.ortega@utp.ac.pa, melany.medina@utp.ac.pa*

[3]Sistema Nacional de Investigación (SNI), Clayton, Panama City, Panama.

[4]Centro de Estudios Multidisciplinarios en Ciencia, Ingeniería y Tecnología (CEMCIT-AIP), Panama City, Panama.

Abstract*– Circular material pathways increasingly rely on biomass residue valorization for bio-based composites, yet early-stage material selection is restricted by conflicting requirements and high variability of natural constituents. This study proposes a traceable screening workflow integrating documentary property evidence with perception-based contextual indicators. A national survey quantified local relevance and operationalized contextual criteria, including availability and perceived environmental impact, to prefilter candidate residue streams. The Analytic Hierarchy Process (AHP) then combined technical criteria (density, tensile strength, Young's modulus, elongation) with contextual criteria to rank fiber and starch-based matrix alternatives. Potato starch ranked first among matrix candidates and remained invariant under analytical breakpoint sensitivity across the admissible weight domain. Fiber ranking identified straw (17.96%), corn husk (15.74%), and sugarcane bagasse (13.72%) as the top alternatives. The selected constituents were propagated to micromechanical screening using the traditional rule of mixtures and a Hirsch-type formulation to estimate Young's modulus and tensile strength ranges for three hybrid composite families: starch–bagasse–straw, starch–bagasse–corn husk, and starch–straw–corn husk. Results provide a decision-to-performance pipeline that narrows the experimental search space and reveals stiffness–strength trade-offs and tolerance to variability across candidate composite families, supporting feasibility-oriented preselection rather than full material qualification. Since the strength of short fiber biocomposites is highly sensitive to microstructural efficiency and interfacial quality, tensile outputs are interpreted as comparative screening indices to guide subsequent controlled fabrication and validation.

Keywords*-- Multicriteria decision making, AHP, bio-based composites, micromechanics, circular economy.

I. Introduction (Heading 1)

The shift from linear production models to regenerative systems has increased interest in the circular economy as a means to reduce resource extraction, minimize environmental impacts, and retain material value through reuse, recycling, and waste stream valorization [1], [2], [3], [4], [5]. Ongoing increases in material throughput, combined with limited end-of-life recovery across numerous product categories, underscore the need for alternative material pathways that decrease reliance on fossil-derived polymers and facilitate localized resource cycles [6], [7].

In this context, biomass residues constitute an underused feedstock relevant to circular material strategies [8], [9]. Agricultural and agro-industrial by-products are produced in significant volumes and are frequently managed through low-value routes such as disposal or open degradation, despite their lignocellulosic composition and potential for reinforcement in polymeric systems [6], [10]. Transforming these residues into composite materials can generate value and alleviate disposal pressures, provided that the resulting materials satisfy application-specific performance and processing requirements and that their end-of-life management is clearly defined [11], [12], [13], [14].

Bio-based composites, particularly those combining natural reinforcements with biopolymer or bio-derived matrices, are often considered promising for sustainable product development due to their potential to reduce embodied impacts and to offer diversified sourcing options compared with conventional glass-fiber composites [14], [15], [16], [17], [18]. However, achieving equivalent performance is not assured. Natural systems typically exhibit greater variability in properties due to differences in fiber morphology, chemistry, moisture sensitivity, interfacial quality, and processing history. These factors introduce trade-offs among stiffness, strength, durability, and manufacturability, complicating direct comparisons among them and with conventional composites [19], [20].

Given these trade-offs, residue-to-composite design extends beyond mechanical optimization to encompass decision-making under multiple, and sometimes conflicting, criteria. In practice, selecting suitable fibers and matrices, especially in the context of the circular economy, involves balancing mechanical targets, such as stiffness and strength, with constraints including availability of residues, environmental relevance, local handling feasibility, and stakeholder acceptance [21]. Multi-criteria decision-making methods (MCDM) are particularly appropriate in this context, as they provide a transparent approach to integrating diverse criteria and systematically documenting how evidence and preferences inform the ranking of alternatives [6], [22].

Among MCDM methods, the Analytic Hierarchy Process (AHP) is widely used to synthesize expert and stakeholder judgments through pairwise comparisons, generating prioritized rankings with internal consistency checks [23]. When integrated with structured literature data, AHP facilitates traceable screening of material options while accommodating contextual criteria beyond purely technical considerations [24]. Concurrently, first-order micromechanical models serve as a pre-validation tool, translating constituent-level selections into projected composite-level stiffness and tensile properties, thereby narrowing the experimental search space prior to fabrication [25].

Accordingly, this study introduces a traceable screening workflow that integrates documentary property evidence, survey-derived relevance signals reflecting local perceptions and feasibility, and AHP-based ranking for fiber and matrix candidates. The highest-ranked constituents are subsequently advanced to a micromechanical screening stage to estimate ranges of composite-family performance and identify stiffness–strength trade-offs under consistent analytical assumptions. This approach yields a reproducible decision-to-performance pipeline that supports early-stage material selection for bio-based composites, explicitly considering both engineering performance and local relevance indicators.

Despite extensive research on natural-fiber biocomposites, early-stage material selection remains a significant challenge. Feasibility is determined by both mechanical performance and contextual factors such as residue accessibility, environmental relevance, and stakeholder acceptance. Additionally, existing screening methods often do not map ranked constituents into a defined mechanical design space, thereby limiting traceability from decision criteria to the expected composite behavior.

To address this gap, the study integrates survey-derived relevance signals and literature-based property evidence within an AHP framework. The highest-ranked constituents are then connected to a micromechanical screening stage. This workflow provides a transparent and reproducible process from decision-making to performance evaluation, reporting both ranking robustness and composite-family performance ranges under consistent analytical assumptions.

II. Methodology

A. Study design and decision scope

A multicriteria decision framework was employed to prioritize natural composite configurations for sustainable product development. The methodology integrates two evidence streams: documented technical property data and a structured perception survey, which are combined using the Analytic Hierarchy Process (AHP). A hierarchical decision structure is established, encompassing objectives, criteria, and alternatives, with pairwise comparisons used to estimate priorities.

B. Decision Criteria and Alternatives

Technical assessment criteria include density, tensile strength, Young's modulus, and elongation, which represent lightweight performance, load transfer capacity, stiffness, and ductility, respectively, for candidate natural composite systems. Alternatives include natural fibers and matrices, with particular emphasis on locally relevant residues and starch-based binders.

C. Data Collection

The methodological pipeline begins with the collection of documentary data from the technical literature, followed by a population survey designed to capture user or stakeholder preferences regarding candidate residues and environmental perception variables. This approach enables integration of engineering performance evidence with local relevance indicators within a unified multicriteria workflow.

A structured literature review was conducted to compile a database of candidate fibers. The documentary search was conducted using Scopus, Web of Science, and Google Scholar. For each candidate fiber, the dataset included reported properties such as density (ρ), tensile strength (σ_t), Young's modulus (E), elongation at break (ε_b), availability and practical sourcing notes, and environmental relevance indicators reported in the source. Only records with traceable measurement context and comparable units were retained for decision modeling.

A national survey was conducted to capture perception-based indicators relevant to residue prioritization. Two survey items were used in the initial screening: Question 14 identified plant species that generate the highest residue levels in Panama, and Question 16 assessed perceptions of which fiber-type residues have the most significant environmental impact. With a finite population of 4,351,000, a minimum sample of 601 respondents was required at a 95% confidence level. Inclusion criteria specified participants aged 18 years or older with prior familiarity with natural fiber composites.

Survey responses were also used to prefilter candidate residues before the final multicriteria ranking. Specifically, responses regarding the perceived potential of residues informed a shortlist comprising husks, sawdust, banana pseudostems, coconut husks, straw, sugarcane bagasse, and corn husks.

D. AHP Formulation

The AHP model is implemented using pairwise comparison matrices for both criteria and alternatives under each criterion. A simplified Saaty-type preference scale with reciprocal values is applied, in which 5 indicates a strong preference, 3 indicates moderate preference, 1 indicates equal preference, and inverse values represent lower preference [23], [24], [26].

For matrix $A = [a_{ij}]$, local priorities are computed from normalized geometric means:

$$\widetilde{w}_i = \left(\prod_{j=1}^{n} a_{ij}\right)^{1/n}, w_i = \frac{\widetilde{w}_i}{\sum_{k=1}^{n} \widetilde{w}_k} \quad (1)$$

Consistency is evaluated through the principal eigenvalue λ_{max}, the consistency index, and the consistency ratio:

$$CI = \frac{\lambda_{\max} - n}{n-1}, RCI = 1.98\frac{(n-2)}{n}, CR = \frac{CI}{RCI} \quad (2)$$

Following the adopted acceptance criterion, a comparison matrix is considered consistent when $CR < 0.10$; otherwise, pairwise judgments are revised until the threshold is met. After the criterion and the alternative weights are obtained for each criterion, global scores are computed via weighted aggregation to produce the final ranking of candidate materials.

E. Priority Synthesis and Ranking

Global priorities are determined by aggregating the criteria weights with the local priorities of alternatives. This process is conducted separately for binder and fiber selection, and the results are consolidated into a final ranked set of candidate material combinations for subsequent prototyping or validation. Traceability is maintained from raw inputs to final ranking by preserving pairwise matrices, weights, and consistency indicators. After validating each pairwise matrix ($CR < 0.10$), local priorities are aggregated to obtain a global score for each alternative. Let W_j be the weight of criterion j, and P_{ij} the local priority of alternative $i$under criterion j. The global priority is computed as:

$$G_i = \sum_{j=1}^{m} W_j \, P_{ij} \qquad (3)$$

where m is the number of criteria. Alternatives are ranked in descending order of G_i. This aggregation was applied separately to matrix and fiber candidates, consistent with the workflow for starch and fiber selection using hierarchical AHP decision matrices. To maintain traceability, the study reports: criteria comparison matrix, local alternative matrices per criterion, CI, RI, and CR values, and final ranking vectors.

Consequently, results are interpreted as a multicriteria-supported preselection and feasibility-oriented evaluation, rather than as full material qualification.

F. Strategy for Selecting Candidate Material Combinations

Following multicriteria prioritization, candidate combinations were generated by pairing the highest-ranked matrix options with the leading fiber streams, while considering practical feasibility constraints. Three hybrid compound families were defined for the analytical stage. This approach translated ranking outcomes into physically interpretable design candidates for subsequent micromechanical prediction.

Analytical micromechanical models were used to estimate composite-level stiffness and tensile strength prior to fabrication, using constituent properties extracted from the literature. This screening step provides a traceable link from constituent selection to the expected mechanical response and supports down-selection prior to experimental validation.

As a first-order estimate, the traditional rule of mixtures (ROM) was used to predict the composite Young modulus:

$$E_c^{ROM} = V_m E_m + V_f E_f \qquad (4)$$

where E_c is the composite Young modulus, E_m and E_f are the Young moduli of the matrix and fiber, and V_m and V_f are their volumetric fractions. The volumetric fractions satisfy:

$$V_f = 1 - V_m \qquad (5)$$

The ROM formulation is generally most accurate for continuous, aligned reinforcements, but it can overestimate stiffness for short, dispersed fibers due to nonideal load transfer and orientation effects.

To account for short-fiber dispersion and non-ideal stress transfer, the Hirsch formulation was adopted for stiffness prediction by combining parallel and series load-sharing contributions:

$$E_c^{Hirsch} = x\left(V_f E_f + V_m E_m\right) + (1 - x)\left(\frac{E_m E_f}{V_f E_m + V_m E_f}\right) \qquad (6)$$

where $x \in [0,1]$ is a load-transfer parameter that reflects the efficiency of matrix–fiber stress transfer. In this study, $x = 0.09$ was used as a representative value for short, dispersed fiber systems, consistent with prior applications of the Hirsch approach to non-continuous reinforcements.

Tensile strength was not computed using the Hirsch model. Instead, a short-fiber load-transfer formulation was used, in which the contribution of the reinforcement depends on fiber geometry and an interface-related shear term through the critical fiber length. The critical length was computed as:

$$l_c = \frac{\sigma_f d}{2\tau} \qquad (7)$$

where σ_f is the fiber tensile strength, d is the fiber diameter, and τ is an interfacial shear-related parameter. The composite tensile strength was then estimated using a modified rule-of-mixtures tensile formulation in which the fiber contribution is reduced when the fiber length is not sufficiently larger than l_c. All parameters and screening assumptions used for σ_t are reported explicitly in Table I.

For hybrid composites containing two distinct reinforcements within the same matrix, the mechanical response was estimated by combining the two corresponding fiber–matrix subsystems. Let $E_{(f1/m)}$ and $E_{(f2/m)}$ be the subsystem moduli predicted using Eq. 6 for fiber 1 and fiber 2, respectively. The hybrid modulus was computed as:

$$E_{hyb} = \phi_1 E_{(f1/m)} + \phi_2 E_{(f2/m)}, \phi_1 + \phi_2 = 1 \qquad (8)$$

where $\phi_1$and ϕ_2 represent the relative volumetric contributions of each reinforcement subsystem. In this work, the weighting factors were defined from the reinforcement fractions used in the screening such that:

$$\phi_1 = \frac{V_{f1}}{V_{f1} + V_{f2}}, \phi_2 = \frac{V_{f2}}{V_{f1} + V_{f2}} \qquad (9)$$

An analogous combination rule was used for tensile strength:

$$\sigma_{t,hyb} = \phi_1 \sigma_{t,(f1/m)} + \phi_2 \sigma_{t,(f2/m)} \qquad (10)$$

where $\sigma_{t,(f1/m)}$ and $\sigma_{t,(f2/m)}$ are computed using the tensile formulation adopted in this study (including $l_c$and τ, Eq. 7, and the associated load-transfer assumptions).

For each composite family (MCP, MCM, and MPM), the analytical outputs were computed across the set of evaluated literature variants and the defined composition space for the screening. Reported performance intervals were then constructed as minimum–maximum ranges over all evaluated variants and compositions. These ranges represent a screening envelope for comparative purposes rather than a definitive material qualification.

Tensile-strength values σ_t reported in this study arise from the adopted analytical screening formulation and the constituent-property inputs compiled from the literature. Because hybrid short-fiber systems are strongly affected by orientation dispersion, void content, moisture sensitivity, interfacial degradation, and processing history, the present σ_t outputs are used as comparative screening indices within the explored design space rather than as direct predictions of experimentally measured tensile strength.

The combinations of these three families represent the transition from multicriteria screening to mechanical performance prediction, enabling consistent comparison across candidate systems under uniform analytical assumptions.

A one-parameter sensitivity analysis was performed for matrix selection by varying the tensile-strength weight w_t over $0 \leq w_t \leq 1$, with $w_E = 1 - w_t$. Using the local priorities obtained from pairwise comparisons, global scores were expressed as linear functions $S_i(w_t)$. Pairwise crossover points were computed by solving $S_A(w_t) = S_B(w_t)$. At the micromechanical stage, sensitivity was quantified using a relative spread metric:

$$\Delta_r = \frac{\max - \min}{\min} \times 100\% \quad (11)$$

computed from the reported ranges for each family. A framework describing the methodology pipeline is depicted in Fig. 1.

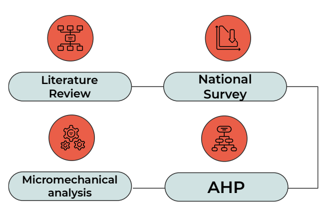

Fig. 1 Framework summarizing the decision-to-performance pipeline.

III. RESULTS

A. *Survey results*

The survey phase provided context-specific relevance indicators to inform the subsequent analytical ranking. The study obtained 684 valid responses, exceeding this threshold. This sample size yields an approximate 95% confidence interval with a half-width of 3.75% for proportion estimates, assuming maximum variability, thereby supporting statistically reliable population-level inference.

Food waste emerged as the most significant type of residue, followed by fruit peels and plant stems. This distribution suggests that respondents prioritized waste streams perceived as both abundant and closely linked to daily activities. Among the selection criteria, sustainability (29%) and availability (25%) were rated as most important, followed by biodegradability (17%). Environmental impact and mechanical properties each received 14%. These results support adopting a multicriteria framework that integrates technical performance with contextual feasibility.

The survey further evaluated perceptions and readiness regarding a circular economy framework. When asked whether organic waste generates environmental impacts, 279 respondents (40.8%) answered affirmatively, and 405 respondents (59.2%) answered negatively. Among respondents who provided justifications for perceived impacts, the dominant qualitative themes were nuisance odors, perceived disease risk, and environmental contamination. This gap motivates the explicit inclusion of sustainability and impact-related criteria in the decision model and highlights the need for clear communication of environmental externalities in waste valorization pathways.

Self-reported familiarity with circular economy concepts was generally low to intermediate. Most respondents indicated basic knowledge (31%) or no knowledge (21%), and 24% did not respond. Despite the limited conceptual familiarity reported, circular economy practices were briefly explained to respondents prior to the question on daily-life behavior. After this clarification, respondents reported engaging in both circular-economy and linear-economy practices. Specifically, 457 respondents (66.8%) selected the circular economy option, and 404 respondents (59.1%) selected the linear economy option; multiple selections were permitted. This outcome suggests that circularity-aligned behavior or preferences may be present even when formal conceptual awareness is limited, supporting the integration of stakeholder-derived relevance signals into the decision framework.

Survey-derived local priorities guided the operationalization of contextual criteria in the decision model, specifically availability and perceived environmental impact. These priorities were summarized in an availability–impact map (Fig. 2), which identifies candidate residue streams that are both accessible and environmentally significant. This approach reinforces the rationale for including these streams in subsequent multicriteria and micromechanical analyses.

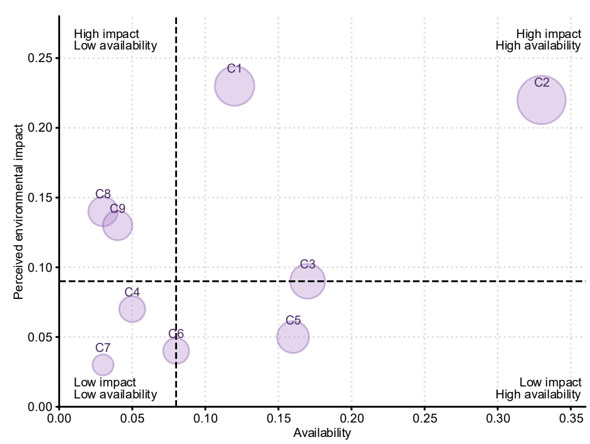

Fig. 2 Availability–impact map of survey-based residue priorities. Dashed lines indicate the median values used to define the four quadrants: high impact–low availability (upper-left), high impact–high availability (upper-right), low impact–low availability (lower-left), and low impact–high

availability (lower-right). Marker size is proportional to the mean of the two priorities, providing a combined indication of overall relevance.

B. *AHP-based prioritization*

B.1. Fiber alternatives

The AHP consistency checks for the fiber-level pairwise comparisons remained within acceptable limits. The consistency ratio was 0.0610 for the Young modulus matrix and 0.0960 for the tensile-strength matrix, both below the 0.10 threshold. The resulting criterion weights assigned the largest contributions to tensile strength and Young modulus (approximately 0.40 each), followed by availability (0.12) and perceived environmental impact (0.08). The global ranking identified three top fiber candidates: C3 (straw, 17.96%), C6 (corn husk, 15.74%), and C9 (sugarcane bagasse, 13.72%) (Figure 3).

B.2. Matrix alternatives

A second AHP stage was used for starch-based matrices (corn, potato, cassava), in which local priorities for tensile strength and Young's modulus were estimated from pairwise comparisons. The tensile matrix reported local priorities of 0.244 (corn), 0.449 (potato), and 0.307 (cassava), with CR = 0.0686. For Young modulus, local priorities were 0.152 (corn), 0.704 (potato), and 0.144 (cassava), with CR = 0.0257. Using reported criterion weights of 0.75 for tensile strength and 0.25 for the Young's modulus, the global matrix scores were 0.513 (potato starch), 0.266 (cassava starch), and 0.220 (corn starch). The selected matrix candidates were potato starch (Matrix 1) and cassava starch (Matrix 2). Results are shown in Figure 4.

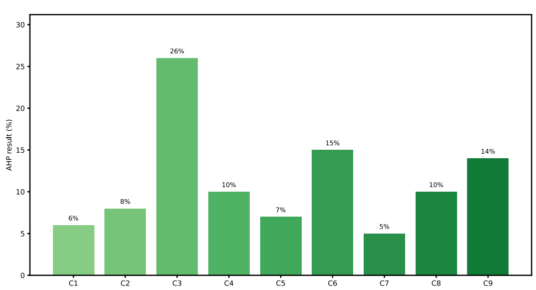

Fig. 3 AHP percentage scores for fiber candidates (C1–C9), where C1, sawdust; C2, peels; C3, straw (grass); C4, palm bark; C5, banana stem; C6, corn husk; C7, corn bagasse; C8, coconut husk; C9, sugarcane bagasse.

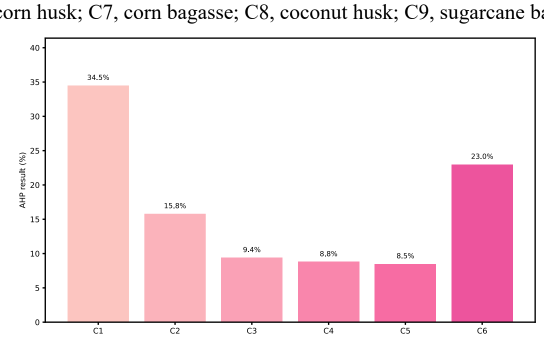

Fig. 4 AHP percentage scores for matrix candidates (C1–C6), where C1, potato starch; C2, cassava starch; C3, rice starch; C4, banana flour; C5, corn starch; C6, sweet potato starch.

Regarding the sensitivity analysis, using the reported local priorities for starch candidates, pairwise crossover points were $w_t = 1.34$ for potato versus cassava and $w_t = 1.59$ for potato versus corn, both outside the feasible domain. Therefore, potato starch remains rank one across the full admissible weight space. A secondary crossover was observed at $w_t = 0.113$ for cassava versus corn, affecting only the second and third ranks. At baseline weights ($w_t = 0.75$), the scores are consistent with the reported ranking: potato 0.513, cassava 0.266, and corn 0.220.

Figure 5 denotes the robustness of the AHP ranking under three weighting scenarios: Baseline, Mechanical, and Sustainability. Baseline denotes the reference weighting scheme based on the original criterion weights. Mechanical and Sustainability scenarios were obtained through controlled weight perturbations followed by renormalization. The heatmap reports the rank of each alternative across scenarios, with rank 1 indicating the highest priority. In matrix selection, C1 remained in first place across all scenarios, followed by C6 and C2. In fiber selection, C3 consistently remained first, followed by C6 and C9. Ranking changes were concentrated among lower-priority alternatives, indicating that perturbations in the weights affected secondary ordering without altering the dominant candidates. These results confirm that the decision framework is robust at the top of the ranking and suitable for downstream micromechanical analysis.

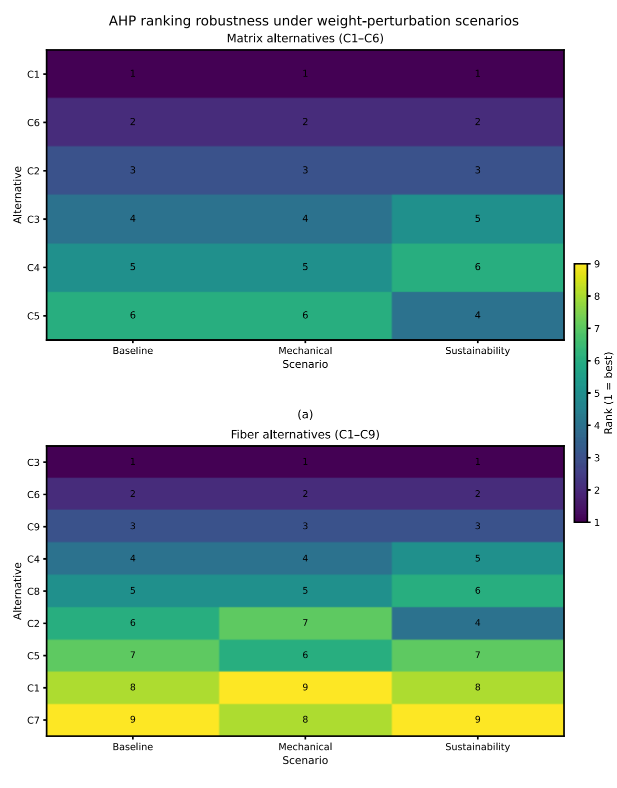

Fig. 4 AHP ranking robustness underweight-perturbation scenarios, showing rank positions across Baseline, Mechanical, and Sustainability scenarios, where rank 1 indicates the highest priority. Panel (a) corresponds to matrix alternatives C1 to C6, and panel (b) corresponds to fiber alternatives C1 to C9.

TABLE I
LITERATURE-DERIVED ELASTIC, STRENGTH, INTERFACIAL, AND GEOMETRIC INPUTS FOR MICROMECHANICAL SCREENING OF SELECTED MATRIX AND FIBER CANDIDATES [27], [28], [29],[30], [31], [29], [30], [31], [32], [33], [34], [35], [36], [37], [38], [39], [40], [41], [42].

Material	E (GPa)	σt (MPa)	τ (MPa)	L (mm)	d (mm)
Potato starch	0.0223	7.90	—	—	—
	0.0040	—	—	—	—
	0.0013	1.03	—	—	—
	0.0009	21.95	—	—	—
Sugarcane bagasse	17.00	235.00	135.68	1.00	0.0020
	23.40	155.00	89.49	1.00	0.0020
	16.32	208.40	120.32	1.00	0.0020
	2.72	27.00	15.59	1.00	0.0020
	5.18	23.30	13.45	1.00	0.0020
	—	169.50	97.86	1.00	0.0020
Kans grass straw fiber	9.60	448.50	258.94	10.00	0.3540
	8.91	337.00	194.57	10.00	0.3540
Corn husk fiber	4.57	160.49	92.66	10.00	0.1000

C. *Micromechanical test and composite-level comparison*

The composite response was predicted using two complementary micromechanical formulations: the traditional rule of mixtures and a modified Hirsch approach that accounts for short-fiber dispersion and non-ideal load transfer. Model inputs included the matrix and fiber elastic moduli, tensile strengths, volumetric fractions, fiber geometry (length and diameter), and interface-related transfer terms. The principal mechanical characteristics of these materials are gathered in Table I. Outputs were Young's modulus and tensile strength for each candidate configuration. The study reports micromechanical evaluations across mixed-fiber families, including MCP (matrix-cane-straw), MCM (matrix-cane-corn), and MPM (matrix-straw-corn), and estimates stiffness and tensile response using analytical formulations.

The composite-level comparison revealed differentiated mechanical profiles among the three families. MCP showed the broadest and highest upper performance window, with predicted Young's modulus ranges of 6.14–16.52 GPa (traditional) and 0.56–1.59 GPa (modified), and tensile strength of 219.60–324.56 MPa. MCM exhibited a wider dispersion with lower tensile response (106.65–163.43 MPa), while MPM presented narrower stiffness ranges (6.43–6.88 GPa traditional; 0.58–0.72 GPa modified) and high tensile performance (241.55–316.88 MPa). The matrix-cane-corn family showed competitive stiffness but had lower tensile performance than matrix-straw-corn in the reported ranges. The matrix-straw-corn family showed a narrower stiffness window with comparatively high tensile values. These outcomes indicate a clear stiffness-strength trade-off across hybrid combinations and support candidate prioritization for subsequent experimental validation. These differences indicate that family-level selection is not governed by a single "best" candidate, but by the required balance between stiffness targets, tensile demand, and variability tolerance.

The micromechanical stage reframes multicriteria ranking as a design-space problem: MCP is favorable when maximizing upper-bound stiffness and strength is prioritized, MPM when a more stable stiffness interval with high tensile response is preferred, and MCM as a lower-strength yet still feasible route, depending on processing and availability constraints. Therefore, the contribution is not only to rank alternatives but also to quantify how each hybrid family behaves mechanically under shared assumptions, thereby improving traceability from decision criteria to expected composite performance.

To avoid overstatement, these results should be interpreted as analytical preselection outcomes rather than full material qualification. The analytical stage reduces design uncertainty and narrows the experimental search space while preserving traceability from ranking assumptions to predicted mechanical behavior.

At the micromechanical stage, for the modified Young modulus, the relative spread was 184% for MCP (0.56 to 1.59 GPa), 387% for MCM (0.31 to 1.51 GPa), and 24% for MPM (0.58 to 0.72 GPa). For tensile strength, the relative spread was 48% for MCP (219.60 to 324.56 MPa), 53% for MCM (106.65 to 163.43 MPa), and 31% for MPM (241.55 to 316.88 MPa). These results indicate that stiffness predictions are most sensitive in MCM and most stable in MPM, whereas the tensile response is comparatively less variable but still composition-dependent.

Figure 5 consolidates the micromechanical screening outcomes at the composite-family level (MCP, MCM, and MPM). For each family, the Young modulus E is reported using both the traditional rule of mixtures (ROM) and the Hirsch formulation, while tensile strength σ_t is reported using the tensile-strength formulation applied in this study, which incorporates load-transfer and fiber-geometry effects. The plotted intervals represent the minimum–maximum ranges observed across the evaluated variants and compositions, and the diamond markers denote the midpoint of each range. Under the Hirsch formulation, MCP reaches the highest upper bound in stiffness (0.56–1.59 GPa) while also exhibiting the highest tensile-strength range (219.60–324.56 MPa). MPM exhibits a comparatively narrow stiffness range (0.58–0.72 GPa) and high tensile strength (241.55–316.88 MPa), indicating more reliable stiffness predictions within the screened domain. In contrast, MCM exhibits the broadest stiffness range (0.31–1.51 GPa) and the lowest tensile-strength region (106.65–163.43 MPa), suggesting higher sensitivity of stiffness predictions to the selected variants and assumptions within the explored space.

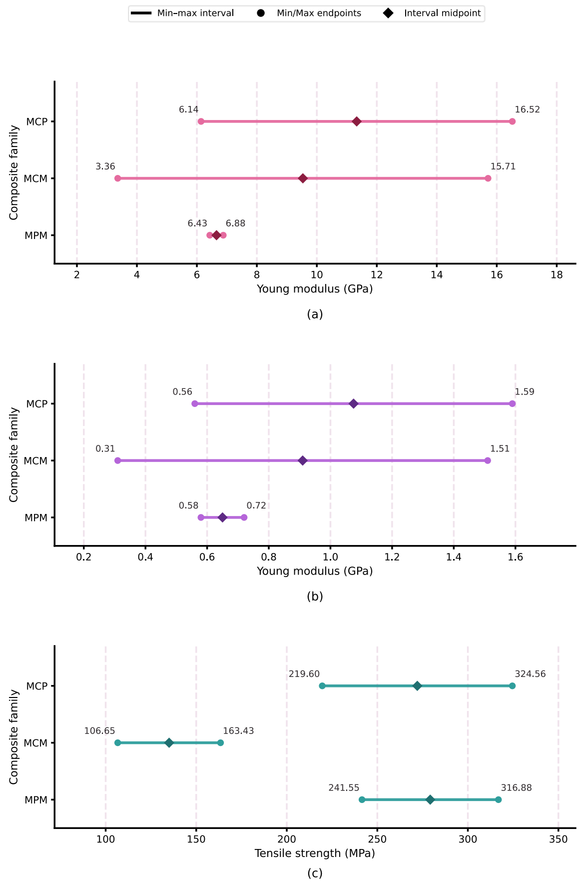

Fig. 5 Global micromechanical performance ranges by composite family. (a) Young's modulus estimated with the traditional rule of mixtures. (b) Young's modulus estimated with the modified micromechanical model, Hirsch type for modulus prediction. (c) Tensile strength is estimated using a modified load-transfer model that accounts for critical fiber-length effects.

Figure 6 summarizes the micromechanical screening by mapping the predicted stiffness–strength trade-off for the three composite families (MCP, MCM, and MPM). Each family is represented as a min–max range in the E–σ_t space, where the shaded box spans the minimum and maximum predicted values obtained across the evaluated variants and compositions, and the diamond marker denotes the range midpoint. In panel (a), the Young modulus is predicted using the Hirsch formulation, whereas panel (b) reports it from the traditional rule of mixtures; in both panels, σ_t is computed using the same tensile-strength formulation applied in this study, which accounts for load transfer and fiber-geometry effects. Overall, MCP occupies the most favorable region of the combined stiffness-tensile strength space, indicating the most balanced mechanical potential among the screened families. MPM exhibits comparatively high tensile strength and a narrower stiffness range, suggesting more stable stiffness predictions across the explored domain. In contrast, MCM exhibits the broadest stiffness range and the lowest tensile-strength region, indicating higher sensitivity of predicted stiffness to the selected variants and inputs and reduced competitiveness in tensile response within the screened space.

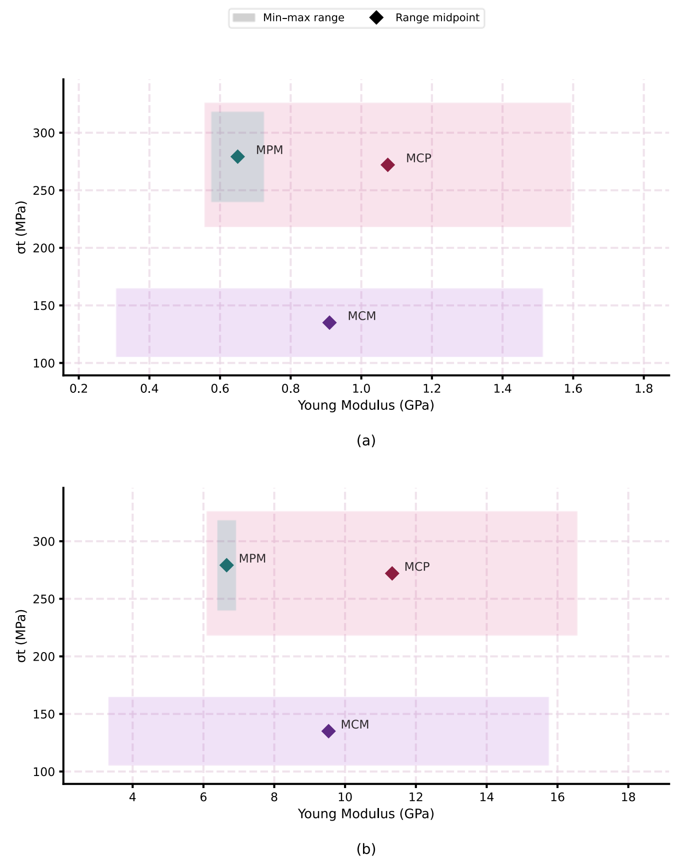

Fig. 6 Performance map relating Young Modulus and tensile strength σ_t for the analytically screened composite families (MCP, MCM, and MPM). (a) Young modulus predicted with the Hirsch model. (b) Baseline Young's modulus was predicted using the traditional rule of mixtures (ROM). Shaded boxes indicate the min–max range of predicted values.

To complement the global performance ranges, Figure 7 provides a compact sensitivity view of the micromechanical outputs using a range-based approach. For each composite family, the minimum and maximum predicted values were converted into relative deviations around the midpoint, enabling a direct comparison of variability in predicted Young Modulus E and tensile strength σ_t across MCP, MCM, and MPM. This visualization enhances the robustness of the discussion by indicating which families exhibit the greatest uncertainty spread between stiffness and strength across the explored screening space.

To contextualize the micromechanical screening ranges, the predicted stiffness and strength were benchmarked against experimental values reported for comparable bio-based composite systems. For starch-based matrices reinforced with lignocellulosic residues, tensile strength is commonly reported in the single-digit megapascal range, with elastic modulus typically below 0.5 GPa; for instance, chemically modified starch reinforced with sugarcane bagasse reached approximately 5 MPa in tensile strength and approximately 0.459 GPa in Young modulus under the processing conditions and fiber loading reported by Mahmud et al. [43]. Ali et al. reported tensile strengths of 0.83 – 1.73 MPa and tensile moduli of 6.71 – 44.36 MPa for thermoplastic starch–bagasse systems across different bagasse loadings [44], while Barboza et al. [45] reported tensile strength near 2.0 MPa and tensile modulus near 70.2 MPa for thermoplastic-starch biocomposites derived from coffee husk and mineral residues.

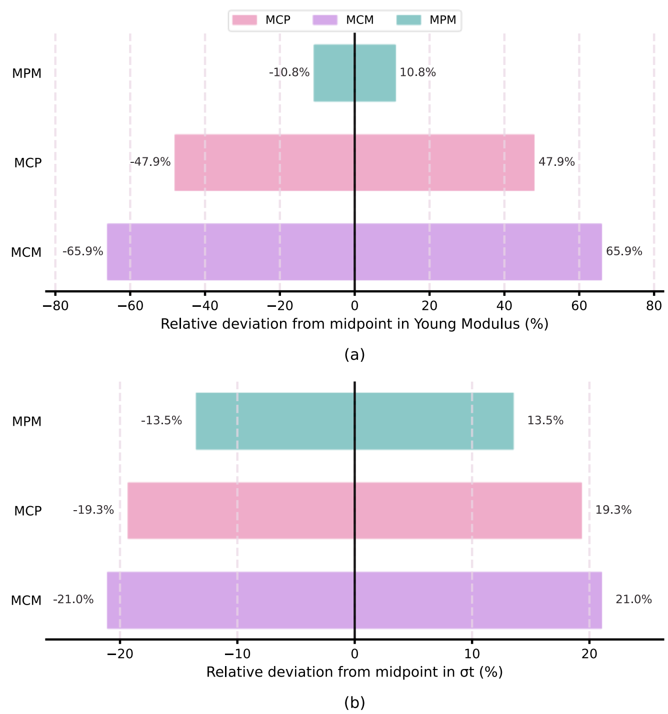

Fig. 7 Range-based micromechanical sensitivity shown as tornado plots for the composite families MCP, MCM, and MPM. (a) Young modulus, E (Hirsch formulation). (b) Tensile strength σ_t (tensile-strength formulation adopted in this study).

In contrast, PLA-based natural-fiber composites can achieve substantially higher stiffness. Experimental evidence indicates that fiber reinforcement can nearly double the modulus, whereas tensile strength may be less responsive, depending on interfacial adhesion, dispersion, and defect content. More broadly, review data indicate that many plant-based natural fiber reinforced composites exhibit maximum tensile strengths in the range of 20–140 MPa and tensile moduli in the range of 1–10 GPa, while also highlighting strong property scatter arising from fiber heterogeneity, moisture uptake, fiber–matrix incompatibility, and processing variability [16]. Peng et al. reported a tensile strength of 31.78 MPa for a 30 wt.% bagasse composite, with a tensile modulus of 219.49 MPa [46].

Reported mechanical properties for biocomposites vary substantially across studies due to differences in botanical source, extraction route, fiber morphology, moisture content, dispersion quality, and interface conditions, which can substantially alter measured properties even for nominally similar formulations. In addition, first-order analytical formulations can overestimate tensile strength when reductions in microstructural efficiency are not explicitly accounted for. For this reason, the present strength values are discussed as upper-bound screening results supporting comparative ranking across the three hybrid families, while experimental validation is required to establish application-specific performance. Accordingly, the present micromechanical outputs should be interpreted as screening-level indicators and upper-bound trends under the adopted assumptions, rather than as direct one-to-one predictions of as-manufactured tensile strength.

IV. Conclusions and Final Remarks

A traceable screening workflow is introduced for early-stage selection of bio-based composite constituents within circular-economy constraints. Contextual feasibility is operationalized through survey-derived relevance signals, specifically addressing availability and perceived environmental impact. Mechanical evidence from documentary sources is integrated using the Analytic Hierarchy Process (AHP) to rank fiber and starch-based matrix candidates with explicit consistency control. The AHP results indicate robust top-ranking alternatives underweight-perturbation scenarios, supporting the stability of the decision stage and justifying progression to analytical screening.

Micromechanical modeling translates constituent-level selections into composite-family performance ranges, enabling comparison of stiffness-strength trade-offs across hybrid families (MCP, MCM, and MPM) under uniform assumptions. The findings indicate that hybrid family selection depends on the targeted balance between stiffness and tensile demands, as well as tolerance to variability, rather than a single dominant option. The proposed decision-to-performance pipeline narrows the experimental search space while maintaining transparency and reproducibility from inputs to ranked outputs and predicted performance ranges.

The outcomes represent analytical preselection rather than comprehensive material qualification. Natural reinforcements and starch-based binders exhibit substantial variability across sources and processing routes. The micromechanical predictions provide screening ranges based on literature-derived property inputs and simplified load-transfer assumptions. Notably, tensile-strength estimates in short-fiber systems are highly sensitive to fiber geometry, orientation efficiency, interfacial conditions, moisture content, and porosity, which are not fully captured in first-order formulations.

Future work should validate the highest-ranked configurations through controlled fabrication and testing, including standardized specimen preparation, moisture conditioning, and statistical replication. Microstructural characterization will be conducted to quantify fiber dispersion and interfacial quality. In parallel, the micromechanical stage will be strengthened by (i) quantifying fiber orientation and length-efficiency factors relevant to short-fiber reinforcement, (ii) measuring or conservatively bounding the interfacial shear strength using standardized tests, and (iii) propagating uncertainty in constituent properties into confidence bands for E and σ_t, enabling conservative design allowables. Finally, the framework will be expanded to incorporate explicit end-of-life pathways, including biodegradation performance metrics under defined conditions, and uncertainty-aware decision modeling to improve applicability to circular material development and localized waste valorization.

ACKNOWLEDGMENT

The authors express their gratitude to the Research Group in Design, Manufacturing, and Materials (DM + M) and the research group Iniciativa De Inegración De Tecnologías para el Desarrollo De Soluciones Ingenieriles (i2tedsi) at the Technological University of Panama (https://utp.ac.pa/, accessed on 28 January 2026) for their collaboration. They also acknowledge support from the National Research System (SNI) and administrative assistance from the Centro de Estudios Multidisciplinarios en Ciencia, Ingeniería y Tecnología (CEMCIT-AIP). Special thanks go to the colleagues from Lab 1-317 for their encouragement and support during this project. This research was funded by the Panamanian Bureau of Science, Technology, and Innovation (Secretaría Nacional de Ciencia, Tecnología e Innovación, SENACYT) under grant IDDS25-30 and grant FIED22-13.

REFERENCES

[1] L. A. Bertolucci Paes, B. S. Bezerra, D. Jugend, et F. Liar Agudo, « Navigating challenges and opportunities in urban circular bioeconomy: A comprehensive review and future directions », *Environmental Development*, vol. 51, p. 101039, sept. 2024, doi: 10.1016/j.envdev.2024.101039.

[2] Y. Bernabé, « Bioeconomía, una herramienta para el desarrollo económico de América Latina », www.laestrella.com.pa. Consulté le: 16 août 2024. [En ligne]. Disponible sur: https://www.laestrella.com.pa/economia/bioeconomia-una-herramienta-para-el-desarrollo-economico-de-america-latina-IK6941820

[3] M. Calisto Friant, K. Reid, P. Boesler, W. J. V. Vermeulen, et R. Salomone, « Sustainable circular cities? Analysing urban circular economy policies in Amsterdam, Glasgow, and Copenhagen », *Local Environment*, vol. 28, nº 10, p. 1331-1369, oct. 2023, doi: 10.1080/13549839.2023.2206643.

[4] P. M. Stathatou, L. Corbin, J. C. Meredith, et A. Garmulewicz, « Biomaterials and Regenerative Agriculture: A Methodological Framework to Enable Circular Transitions », *Sustainability*, vol. 15, nº 19, sept. 2023, doi: 10.3390/su151914306.

[5] A. S. Milani et M. Takaffoli, *Biocomposites and the Circular Economy*. Woodhead Publishing, 2025.

[6] I. Enriquez-Medina, I. Rodas-Ortiz, I. Bedoya-Garcia, A. Velasquez-Godoy, C. Alvarez-Vasco, et A. Ceballos Bermudez, « Bridging gap between agro-industrial waste, biodiversity and mycelium-based biocomposites: Understanding their properties by multiscale methodology », *Journal of Bioresources and Bioproducts*, vol. 9, nº 4, p. 495-507, nov. 2024, doi: 10.1016/j.jobab.2024.07.001.

[7] S. Afsar, A. T. Estevez, Y. K. Abdallah, G. D. Turhan, B. Oze, et A. Doyuran, « Activating Co-Creation Methodologies of 3D Printing with Biocomposites Developed from Local Organic Wastes », présenté à Proceedings of the International Conference on Education and Research in Computer Aided Architectural Design in Europe, 2022, p. 215-224. [En ligne]. Disponible sur: https://www.scopus.com/inward/record.uri?eid=2-s2.0-85139744746&partnerID=40&md5=7f2ff7846f52a643f8b2c435f5e80f8e

[8] M. Tanase-Opedal, E. Espinosa, A. Rodríguez, et G. Chinga-Carrasco, « Lignin: A Biopolymer from Forestry Biomass for Biocomposites and 3D Printing », *Materials*, vol. 12, nº 18, p. 3006, janv. 2019, doi: 10.3390/ma12183006.

[9] V. Shanmugam *et al.*, « Circular economy in biocomposite development: State-of-the-art, challenges and emerging trends », *Composites Part C: Open Access*, vol. 5, p. 100138, juill. 2021, doi: 10.1016/j.jcomc.2021.100138.

[10] N. Giani *et al.*, « Valorization of Agro-Wastes as Fillers in PLA-Based Biocomposites for Increasing Sustainability in Fused Deposition Modeling Additive Manufacturing », *Materials*, vol. 17, nº 6, mars 2024, doi: 10.3390/ma17061421.

[11] M. P., S. V. K, V. P. Elanjeitsenni, et A. J. G, « Valorisation of corn waste as fiber, biosilica, and their epoxy composites: fatigue, fracture toughness, water absorption, and drilling properties », *Biomass Conv. Bioref.*, vol. 15, nº 11, p. 16891-16903, juin 2025, doi: 10.1007/s13399-024-06306-6.

[12] A. Sholokhova, V. Varžinskas, et R. Rutkaitė, « Valorization of Agro-waste in Bio-based and Biodegradable Polymer Composites: A Comprehensive Review with Emphasis on Europe Perspective », *Waste Biomass Valor*, vol. 16, nº 4, p. 1537-1571, avr. 2025, doi: 10.1007/s12649-024-02856-y.

[13] P. Rana et S. Sethi, « Utilising Agro-waste in Textile Industry: Advancing Sustainability with a Year-Round Waste Cycle », *Mater Circ Econ*, vol. 7, nº 1, p. 30, août 2025, doi: 10.1007/s42824-025-00188-3.

[14] « Agri-wastes for biocomposites », in *Biocomposites and the Circular Economy*, Woodhead Publishing, 2025, p. 13-25. doi: 10.1016/B978-0-443-23718-8.00002-8.

[15] P. Anerao, A. Kulkarni, et Y. Munde, « A review on exploration of the mechanical characteristics of 3D-printed biocomposites fabricated by fused deposition modelling (FDM) », *Rapid Prototyping Journal*, vol. 30, nº 3. p. 430-440, 2024. doi: 10.1108/RPJ-04-2023-0150.

[16] M. Li *et al.*, « Recent advancements of plant-based natural fiber–reinforced composites and their applications », *Composites Part B: Engineering*, vol. 200, p. 108254, nov. 2020, doi: 10.1016/j.compositesb.2020.108254.

[17] M. Adamu, F. Alanazi, Y. E. Ibrahim, H. Alanazi, et V. C. Khed, « A Comprehensive Review on Sustainable Natural Fiber in Cementitious Composites: The Date Palm Fiber Case », *Sustainability*, vol. 14, nº 11, p. 6691, mai 2022, doi: 10.3390/su14116691.

[18] R. Ahmed, K. H. Manik, A. Nath, J. R. Shohag, J. J. Mim, et N. Hossain, « Recent advances in sustainable natural fiber composites: Environmental benefits, applications, and future prospects », *Materials Today Sustainability*, vol. 32, p. 101220, déc. 2025, doi: 10.1016/j.mtsust.2025.101220.

[19] A. Pavlovic, L. Valzania, G. Minak, A. Pavlovic, L. Valzania, et G. Minak, « Effects of Moisture Absorption on the Mechanical and Fatigue Properties of Natural Fiber Composites: A Review », *Polymers*, vol. 17, nº 14, juill. 2025, doi: 10.3390/polym17141996.

[20] C. I. Madueke, O. M. Mbah, et R. Umunakwe, « A review on the limitations of natural fibres and natural fibre composites with emphasis on tensile strength using coir as a case study », *Polym. Bull.*, vol. 80, nº 4, p. 3489-3506, avr. 2023, doi: 10.1007/s00289-022-04241-y.

[21] H. Corvellec, A. F. Stowell, et N. Johansson, « Critiques of the circular economy », *Journal of Industrial Ecology*, vol. 26, nº 2, p. 421-432, 2022, doi: 10.1111/jiec.13187.

[22] S. Alonso-Cañon, E. Blanco-Fernández, D. Castro-Fresno, A. I. Yoris-Nobile, et L. Castanon-Jano, « Comparison of reinforcement fibers in 3D printing mortars using multi-criteria analysis », *International Journal of Advanced Manufacturing Technology*, vol. 134, nº 3-4. Springer Science and Business Media Deutschland GmbH, p. 1463-1485, 2024. doi: 10.1007/s00170-024-14126-1.

[23] T. L. Saaty, *The Analytic Hierarchy Process: Planning, Priority Setting, Resource Allocation*. New York ; London, 1980.

[24] H. N. Salwa, S. M. Sapuan, M. T. Mastura, et M. Z. Mohamed Yusoff, « Analytic Hierarchy Process (AHP)-based materials selection system for natural fiber as reinforcement in biopolymer composites for food packaging », *BioResources*, vol. 14, nº 4. North Carolina State University lucian.lucia@NCSU.edu, p. 10014-10046, 2019. doi: 10.15376/biores.14.4.10014-10046.

[25] Michael F. Ashby, *Materials Selection in Mechanical Design*. 2016. Consulté le: 14 février 2026. [En ligne]. Disponible sur: https://shop.elsevier.com/books/materials-selection-in-mechanical-design/ashby/978-0-08-100599-6

[26] S. N. M. Farhan Han, M. T. Mastura, M. R. Mansor, S. I. Abdul Kudus, et P. Pradel, « WEIGHTING THE MATERIAL REQUIREMENTS OF NFRC BY USING FUZZY AHP WITH EXTENT ANALYSIS », *Journal of Advanced Manufacturing Technology*, vol. 14, nº 2-2. p. 211-222, 2020.

[27] V. Ahlawat, A. Parinam, et S. Kajal, « Experimental study of tensile and flexural properties of kans grass fiber reinforced polyester composites », *IJEMS Vol.25(4) [August 2018]*, août 2018, Consulté le: 15 juillet 2023. [En ligne]. Disponible sur: http://nopr.niscpr.res.in/handle/123456789/45266

[28] G. L. Devnani et S. Sinha, « Extraction, characterization and thermal degradation kinetics with activation energy of untreated and alkali treated Saccharum spontaneum (Kans grass) fiber », *Composites Part B: Engineering*, vol. 166, p. 436-445, juin 2019, doi: 10.1016/j.compositesb.2019.02.042.

[29] K.-D. González-Velandia, D. Daza-Rey, P.-A. Caballero-Amado, et C. Martínez-González, « Evaluación de las propiedades físicas y químicas de residuos sólidos orgánicos a emplearse en la elaboración de papel. », *luaz*, vol. 43, p. 499-517, mai 2016, doi: 10.17151/luaz.2016.43.21.

[30] S. Hadi et B. A. Sudrajat, « Analysis of Flexural Strength Test Results of Coconut Fiber and Corn Husk Composite for Hanging Rack », *Intek*, vol. 7, nº 1, p. 45, avr. 2020, doi: 10.31963/intek.v7i1.2126.

[31] N. Herlina Sari, I. N. G. Wardana, Y. Surya Irawan, et E. Siswanto, « The Effect of Sodium Hydroxide on Chemical and Mechanical Properties of Corn Husk Fiber », *Orient. J. Chem*, vol. 33, nº 6, p. 3037-3042, déc. 2017, doi: 10.13005/ojc/330642.

[32] Y. Sachin, G. Gourav, et B. Ravi, « A Review on Composition and Properties of Bagasse Fibers », *2015*, vol. 6, nº 5, p. 143-148, 2015.

[33] E. Jayamani, Md. R. Rahman, D. A. Benhur, M. K. B. Bakri, A. Kakar, et A. Khan, « Comparative study of fly ash/sugarcane fiber reinforced polymer composites properties », *BioRes*, vol. 15, nº 3, p. 5514-5531, mai 2020, doi: 10.15376/biores.15.3.5514-5531.

[34] H. Mohit et V. A. M. Selvan, « Thermo-mechanical properties of sodium chloride and alkali-treated sugarcane bagasse fibre », *IJFTR Vol.44(3) [September 2019]*, sept. 2019, Consulté le: 1 juillet 2023. [En ligne]. Disponible sur: http://nopr.niscpr.res.in/handle/123456789/50554

[35] R. M. Rowell, « Natural fibres: types and properties », in *Properties and Performance of Natural-Fibre Composites*, Elsevier, 2008, p. 3-66. doi: 10.1533/9781845694593.1.3.

[36] A. Vázquez, V. A. Domínguez, et J. M. Kenny, « Bagasse Fiber-Polypropylene Based Composites », *Journal of Thermoplastic Composite Materials*, vol. 12, nº 6, p. 477-497, nov. 1999, doi: 10.1177/089270579901200604.

[37] W. J. Mora Espinosa, B. A. Ramón Valencia, et G. G. Moreno Contreras, « Natural fibers as an alternative of reinforcement in composite materials. a review. », *BISTUA*, vol. 17, nº 2, p. 60, août 2019, doi: 10.24054/01204211.v2.n2.2019.3523.

[38] Y. Díaz Herrera, C. A. Villaseñor Perea, A. Pérez López, A. Mancera Rico, M. del R. Venegas Ordoñez, et A. Ramírez Jaspeado, « Elaboración y caracterización físico – mecánica de biocompuestos a base de harina de arroz y fibra de bagazo de caña », *BIOTECNIA*, vol. 24, nº 1, p. 23-29, févr. 2022, doi: 10.18633/biotecnia.v24i1.1468.

[39] A. López-Córdoba, S. Estevez-Areco, et S. Goyanes, « Potato starch-based biocomposites with enhanced thermal, mechanical and barrier properties comprising water-resistant electrospun poly (vinyl alcohol) fibers and yerba mate extract », *Carbohydrate Polymers*, vol. 215, p. 377-387, juill. 2019, doi: 10.1016/j.carbpol.2019.03.105.

[40] R. Farajpour, Z. Emam Djomeh, S. Moeini, H. Tavakolipour, et S. Safayan, « Structural and physico-mechanical properties of potato starch-olive oil edible films reinforced with zein nanoparticles », *International Journal of Biological Macromolecules*, vol. 149, p. 941-950, avr. 2020, doi: 10.1016/j.ijbiomac.2020.01.175.

[41] N. Gürler et G. Torğut, « Graphene-reinforced potato starch composite films: Improvement of mechanical, barrier and electrical properties », *Polymer Composites*, vol. 42, nº 1, p. 173-180, janv. 2021, doi: 10.1002/pc.25816.

[42] A. Romano, V. D'Amelia, V. Gallo, S. Palomba, D. Carputo, et P. Masi, « Relationships between composition, microstructure and cooking performances of six potato varieties », *Food Research International*, vol. 114, p. 10-19, déc. 2018, doi: 10.1016/j.foodres.2018.07.033.

[43] Md. A. Mahmud, N. Abir, S. A. Belal, et Md. A. Gafur, « Chemical characterization and tensile properties of a sugarcane bagasse-chemically modified starch composite structure developed for packaging purposes », *Results in Materials*, vol. 25, p. 100634, mars 2025, doi: 10.1016/j.rinma.2024.100634.

[44] B. Henrique, « Influence of Sugarcane Bagasse Fiber Size on Biodegradable Composites of Thermoplastic Starch », *JRM*, vol. 6, nº 2, p. 176-182, 2018, doi: 10.7569/JRM.2018.634101.

[45] L. S. Barboza *et al.*, « Sustainable Thermoplastic Starch Biocomposites from Coffee Husk and Mineral Residues: Waste Upcycling and Mechanical Performance », *Sustainability*, vol. 17, nº 20, oct. 2025, doi: 10.3390/su17209248.

[46] Y. Peng, W. Lei, W. Yu, et Y. Chen, « Effect of Sugarcane Bagasse Content and Modification on the Properties of Sugarcane Bagasse/Poly(lactic Acid) Biocomposites », *Molecules*, vol. 30, nº 7, avr. 2025, doi: 10.3390/molecules30071583.